Alertness opens the effective flow of sensory information through rat thalamic posterior nucleus

Aleksander Sobolewski,* Ewa Kublik, Daniel A. Swiejkowski,† Jan Kamiński‡ and Andrzej Wróbel
Department of Neurophysiology, Nencki Institute of Experimental Biology, 3 Pasteur Str., Warsaw 02-093, Poland

Abstract

Behavioural reactions to sensory stimuli vary with the level of arousal, but little is known about the underlying reorganization of neuronal networks. In this study, we use chronic recordings from the somatosensory regions of the thalamus and cortex of behaving rats together with a novel analysis of functional connectivity to show that during low arousal tactile signals are transmitted via the ventral posteromedial thalamic nucleus (VPM), a first-order thalamic relay, to the primary somatosensory (barrel) cortex and then from the cortex to the posterior medial thalamic nucleus (PoM), which plays a role of a higher-order thalamic relay. By contrast, during high arousal this network scheme is modified and both VPM and PoM transmit peripheral input to the barrel cortex acting as first-order relays. We also show that in urethane anaesthesia PoM is largely excluded from the thalamo-cortical loop. We thus demonstrate a way in which the thalamo-cortical system, despite its fixed anatomy, is capable of dynamically reconfiguring the transmission route of a sensory signal in concert with the behavioural state of an animal.

Introduction

Thalamic relay neurons have been proposed to participate in two types of thalamocortical circuits (Sherman & Guillery, 1996). The first-order (FO) relays transmit peripheral information to the cortex, while the higher order (HO) relays mediate transthalamic cortico-cortical flow. Whether a thalamic neuron participates in either of these circuits depends on the origin of its driving input. The driving input to a neuron is defined by a number of features, e.g. presence of large excitatory terminals synapsing on proximal dendrites and large and fast excitatory postsynaptic potentials (EPSPs) that undergo paired-pulse depression. Thus, an influence of the driving input on postsynaptic activity is strong, reliable and temporally precise. FO thalamic relays are driven by subcortical structures while HO thalamic relays receive their driving input from cortical layer 5 (for a review see Sherman & Guillery, 2011).

Certain thalamic neurons have been shown to participate in only one of these circuits. For instance, in rats the ventral posteromedial nucleus (VPM) consists of neurons that are contacted by driving inputs originating solely in the somatosensory trigeminal nuclei (Hoogland *et al.*, 1991) and thus VPM is referred to as the FO somatosensory nucleus. By contrast, the somatosensory-responsive medial region of the posterior thalamic nucleus (PoM) has been shown to be a target of driving inputs from both peripheral trigeminal nuclei (Lavallée *et al.*, 2005) and cortical layer 5 of the primary somatosensory (barrel) cortex (Hoogland *et al.*, 1991; Veinante *et al.*, 2000). Recently, the convergence of driving inputs from both the periphery and the cortex was shown also for individual PoM relay neurons (Groh *et al.*, 2014). However, in spite of this mixed character of driving inputs, PoM is commonly regarded as the HO thalamic nucleus due to long latency of evoked somatosensory responses and their disappearance after inactivation of the barrel cortex, which were shown in urethane-anaesthetized rats (Diamond *et al.*, 1992a). The discrepancy between the synaptic features indicating that PoM participates in both FO and HO circuits and widely reported lack of early FO responses of PoM neurons to sensory input in anaesthesia (for a review see Waite, 2004; but see also Ahissar *et al.*, 2000) has been attributed to strong inhibition of PoM by the zona incerta (ZI; Power *et al.*, 1999, 2001; Barthó *et al.*, 2002) or anterior pretectal nucleus (APT; Bokor *et al.*, 2005), which are activated by somatosensory stimulation at short latencies and in turn can shunt the peripheral driving input to PoM (Trageser & Keller, 2004; Lavallée *et al.*, 2005). Inhibition of ZI by cholinergic agents or by electrical stimulation of brainstem cholinergic centres in anaesthetized rats (Trageser *et al.*, 2006) facilitated early PoM responses, which has raised the possibility that the mode of operation of PoM depends on the behavioural state of an animal. To test this hypothesis we have recorded whisker-evoked responses from the barrel cortex, VPM and PoM of rats at three vigilance levels (general anaesthesia, quiescent wakefulness and alertness), and applied a novel method of analysis of functional connectivity.

Correspondence: Dr A. Wróbel, as above.
E-mail: wrobel@nencki.gov.pl.

*Present address: Center for Neuroprosthetics, École Polytechnique Fédérale de Lausanne, CH-1015 Lausanne, Switzerland

†Present address: Anatomical Neuropharmacology Unit, Department of Pharmacology, Medical Research Council, University of Oxford, Oxford OX1 3TH, UK

‡Present address: Division of Biology and Biological Engineering, California Institute of Technology, 1200 E California Blvd, Pasadena, CA 91125, USA

Materials and methods

The experiment

Wistar male rats (n = 5, 300–400 g) were used in this chronic experiment. All procedures followed the 86/609/EEC directive and were approved by the 1st Warsaw Local Ethics Committee.

For 2–3 weeks, the rats were handled and habituated to rest in a restraining knitwear hammock suspended by a velcro tape in a plexiglas frame. Then, under general anaesthesia (chloral hydrate, Sigma-Aldrich, St Louis, MO, USA; 3.6%, 1 mL/100 g body weight), the rats were implanted with electrodes (up to four in the barrel cortex and 12–15 in the thalamus) that were custom made from 25-μm tungsten wire (California Fine Wire, Grover Beach, CA, USA) with gold-plated conically sharpened tips (~150 kΩ impedance at 1 kHz). Wires were glued together to form multi-contact electrode shafts and attached with nickel electro-conductive paint to Microtech female connectors. For the thalamus, three to four shafts made of three to five wires (with inter-tip distance of approximately 0.4 mm) were combined into one multi-electrode, which was aimed to reach simultaneously PoM and VPM nuclei [approximate coordinates for thalamus: AP = 3.0–3.6 mm, L = 3.2 mm, H = −5.8 to −6.2 mm (VPM); L = 2.6 mm, H = −5.4 to −5.6 mm (PoM); barrel cortex: AP = −2.2 mm, L = 5.5 mm, H = −0.7 to −1.5 mm; Paxinos & Watson (2007)]. Implantation was performed under electrophysiological control, i.e. along the implantation track we recorded responses evoked first by visual stimuli (in the laterodorsal and lateral posterior thalamic nuclei) and then by whisker stimulation (at the level of somatosensory thalamus). Stainless steel anchoring screws were inserted into the skull bone, and served as a reference for recording. A socket (with a threaded nut for restraining the head) was secured to the skull using acrylic polymer. For five days after the surgery, the rats received analgesic drugs (carprofen - Rimadyl, Pfizer, New York, USA; 5 mg/kg body weight, s.c.) and an antibiotic (enrofloxacin - Baytril, Bayer, Leverkeusen, Germany; 5 mg/kg body weight, s.c.).

After the recovery period, the animals were subjected to four to eight habituation sessions (1 h per day). Awake rats were as before suspended in the hammock slung from the plexiglas frame but this time with the head securely attached to the frame by a screw fastened to the threaded nut embedded in the acrylic socket. A group of ~20 of their largest facial whiskers were attached (i.e. glued with nail polish to avoid the risk of whisker slippage) to a piezoelectric actuator at a distance of ~20 mm from the snout. We chose multi- and not single-whisker stimulation to activate whole whisker sectors of VPM and PoM to avoid problems with somatotopic misalignment of thalamic and cortical recording locations. PoM cells have larger receptive fields than VPM cells, and thus the somatotopic misalignment would differently influence the signals evoked by single whisker stimulation in the two nuclei.

During each session the whiskers were stimulated 80–120 times with a 1-ms square impulse evoking a down-and-up motion of ~100 μm with a pseudo-random inter-trial interval of 10–45 s. The experimental session, which followed the habituation sessions, consisted of two parts: (1) in the first part (quiescent condition) the rats received 50–60 whisker stimulations in conditions identical to those of the habituation sessions; and (2) in the second part (arousal condition), they received a further 50–60 whisker stimulations, but interleaved with additional arousing stimuli. The above session sequence (several habituation sessions followed by an experimental session) was repeated two to five times for each rat. Arousing stimuli consisted of electric currents (1-s trains of 3-ms square pulses at 50 Hz, 0.03–0.07 mA) applied to the skin of the rat's ear, or (depending on the session) loud sounds (1 s, 7000 Hz, 90 dB) from a speaker positioned 10 cm from the rat's ear. In four rats, an additional session took place in which the whisker stimulations were conducted under urethane (1.5 g/kg body weight, i.p.) anesthesia.

Throughout all sessions, local field potentials (LFPs) were recorded (0.1–5000 Hz band pass filter, amplification ×1000, 10 kHz sampling frequency, Spike 2 software, Power1401 interface, CED, Cambridge, UK) along with a video from a USB camera that had been set up to view the rat's snout (Spike 2 Video Recorder, CED). Immediately after implantation of electrodes, the recorded signal also included action potentials, although during later recovery and habituation this multi-unit activity disappeared from most of the channels.

After completion of the recordings, the rats were injected with an overdose of pentobarbital (150 mg/kg body weight, i.p.) and perfused transcardially with a saline solution followed by a 4% paraformaldehyde solution. Brains were removed, cryoprotected in 30% sucrose, cut into 50-μm slices and stained with cresyl violet and cytochrome oxidase for histological verification of the electrode placement. To conduct further analysis of the electrophysiological signals, we chose one electrode that was located in layer 5 of the barrel cortex and two electrodes that were confirmed to have reached the vibrissal representations in the VPM and PoM of each rat (Fig. 1).

Analysis of LFP data

Dataset

Somatosensory evoked potentials (EPs), i.e. LFP signal epochs of 25 ms beginning at the onset of a vibrissal stimulus from the three selected channels (VPM, PoM, barrel cortex) were exported to Matlab software environment (The MathWorks, Inc., Natick, MA, USA). Epochs that were contaminated by artefacts were rejected, and the remaining EPs were pooled for each behavioural state. The least numerous dataset recorded from one rat contained 160 EPs from the quiescent and 160 EPs from the aroused condition. Thus, to balance the data we analysed an equal number of EPs from every rat. All the EPs taken for the analysis from all rats were pooled together, which resulted in a total of 1600 EPs (800 for both the quiescent and the aroused conditions).

For anaesthetized conditions we had 240 EPs (60 for each rat). All of the EPs were brought to a common baseline by subtracting the potential that was measured at the time of the stimulus delivery and were normalized within each session to a standard score (all samples of each EP were divided by the standard deviation of all the data samples from a given session).

Cross-trial correlation analysis

The aim of this study was to understand how the thalamo-cortical connections function in behaving animals in different brain states. As our fixed wire electrodes could not reliably record single units over a chronic experiment, we could not use methods applied to spike trains (e.g. Joint-PSTH, Aertsen *et al.*, 1989). Neither could we rely on methods working in the frequency domain (e.g. DTF, Korzeniewska *et al.*, 2008; noise correlation, Einevoll *et al.*, 2013) as they assume a dominant oscillatory character of interactions and are less sensitive in the early thalamo-cortical responses investigated by us. Thus, to assess functional connectivity between the thalamus (VPM and PoM) and the barrel cortex in different behavioural
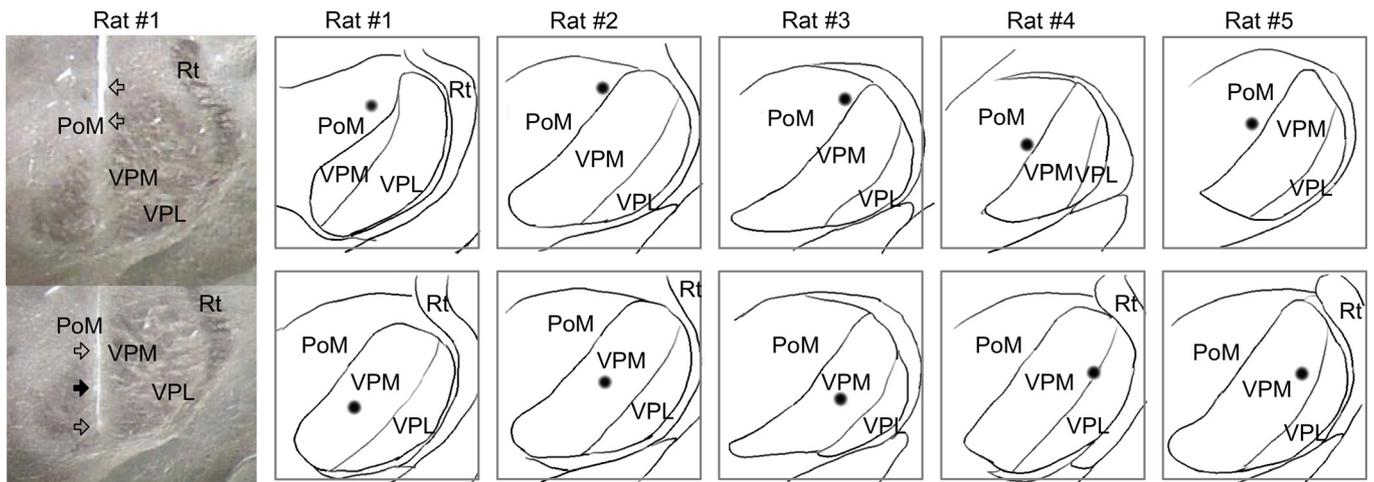
FIG. 1. Histological verification of electrodes locations in a rat (#1) implanted with a thalamic electrode built from three-five-wire shafts. Photographs show low-magnification views of the two neighbouring cytochrome oxidase-stained slices with an electrode's track going through PoM and VPM. Arrows point to the traces of wire tips in PoM (upper photo) and VPM (lower photo, black arrow indicates recording point chosen for VPM analysis in this rat). Schematic drawings indicate recording points for all five rats: PoM – upper row, VPM – lower row. VPM, PoM, see text; VPL, ventral posterolateral nucleus; Rt, reticular nucleus of the thalamus.

conditions (anaesthetized, quiescent, aroused), we used cross-trial correlation (CTC), a method that was developed by Sobolewski *et al.* (2010). Briefly, the method is similar to Joint-PSTH (Aertsen *et al.*, 1989) in that it is applied to responses evoked by a repeated sensory stimulation at two sites and measures stimulus-driven connectivity. While Joint-PSTH works on spike trains of simultaneously recorded neurons, CTC uses the local field potential from simultaneously recorded structures. Spike trains are binary; the repetitive coexistence of spike events (coded as 1) or its lack (coded as 0) in two structures can reliably build up the value of the bins in the JPSTH-matrix, which indicates functional connection. By contrast, in case of LFP, non-zero values always coexist in two analysed time-series. Thus, to estimate the relationship between the signals CTC does not look for the coexistence of particular amplitude values but for covariance of trial-to-trial amplitude increases and decreases (see Fig. 2E). CTC assumes that such trial-to-trial changes should be similar in anatomical structures with a strong functional connection. A large potential evoked at one such structure is followed by a large potential in the recipient structure (at a latency delayed by transmission time) and, analogously, a small response at one site is followed by a small response at the other.

CTC calculates the correlation of two time series (Fig. 2E) containing potential values measured from two structures at particular post-stimulus latencies (Fig. 2C and D). Such calculation is repeated for all combinations of peristimulus time-points and resulting coefficients are presented as a correlation matrix (Fig. 2F). Clusters of significant coefficients indicate the strength (values of the coefficients) and time relationship of the functional interaction (see Figs 2 and 5 where clusters located above the diagonal reflect thalamo-cortical and those located below the diagonal cortico-thalamic influences). Positive coefficients appear when synchronous changes of signal amplitude in two structures are unidirectional, and negative when the amplitudes change in opposite directions. These are only mathematical values – for adequate physiological interpretation one has to take into account a number of other factors: (1) the excitatory or inhibitory character of studied connections; (2) interpretation of consecutive EP waves (see Results); and (3) the well-established anatomy of the thalamo-cortical network of the vibrissal–barrel system. In our application we restricted the analysis to the early post-

stimulus time window (25 ms), for which the results can be unambiguously related to already well-established anatomy.

While the correlation matrix from a single CTC run might not be very striking (simply reflecting existing anatomical pathways), important results come from the comparison of the correlation patterns of the same network at different situations – as in our experiment in which CTC was calculated for VPM–cortex and PoM–cortex pairs, separately for three arousal states (anaesthesia, quiescence, arousal). This allowed us to estimate (with an interpretation based of known connections and activation patterns) the changing efficacy of consecutive stages of thalamo-cortico-thalamic processing.

For the purpose of this report, the CTC method was enhanced with two additional procedures, which are applied here, but were not described in our original methodological paper. The first – a two-dimensional implementation of a cluster-based permutation test (Maris & Oostenveld, 2007; Sobolewski *et al.*, 2011) – was applied to control for false-discovery ('multiple comparisons') errors and at the same time it helped to remove correlations resulting from the co-stimulation of the two structures. The second is a field-effect (electrode 'cross-talk') correction, which was applied to control for possible electrotonic interference between neighbouring recording sites. The CTC matrices presented as main results in Fig. 5 contain only those correlation clusters that survived both the false-discovery and the field-effect corrections.

False-discovery correction

This correction constitutes a two-dimensional implementation (Sobolewski *et al.*, 2011) of the cluster-based permutation procedure originally proposed for one-dimensional (evoked potential) statistical analysis by Maris & Oostenveld (2007). As CTC matrices are constructed by calculating numerous correlation coefficients (on the order of 10^5), random (false) significant correlations can be expected. The correction allows elimination of such false positive discoveries. Its algorithm is as follows:

(1) The sequence of the EPs from one of the locations is randomly permuted and the CTC matrix is recalculated.

(2) All non-significant correlation coefficients, i.e. where $P > 0.01$, are substituted with zeros. The P-values for each correlation

A Thalamic recordings

B Cortical recordings

C Variability vectors

D

Potential [mV]
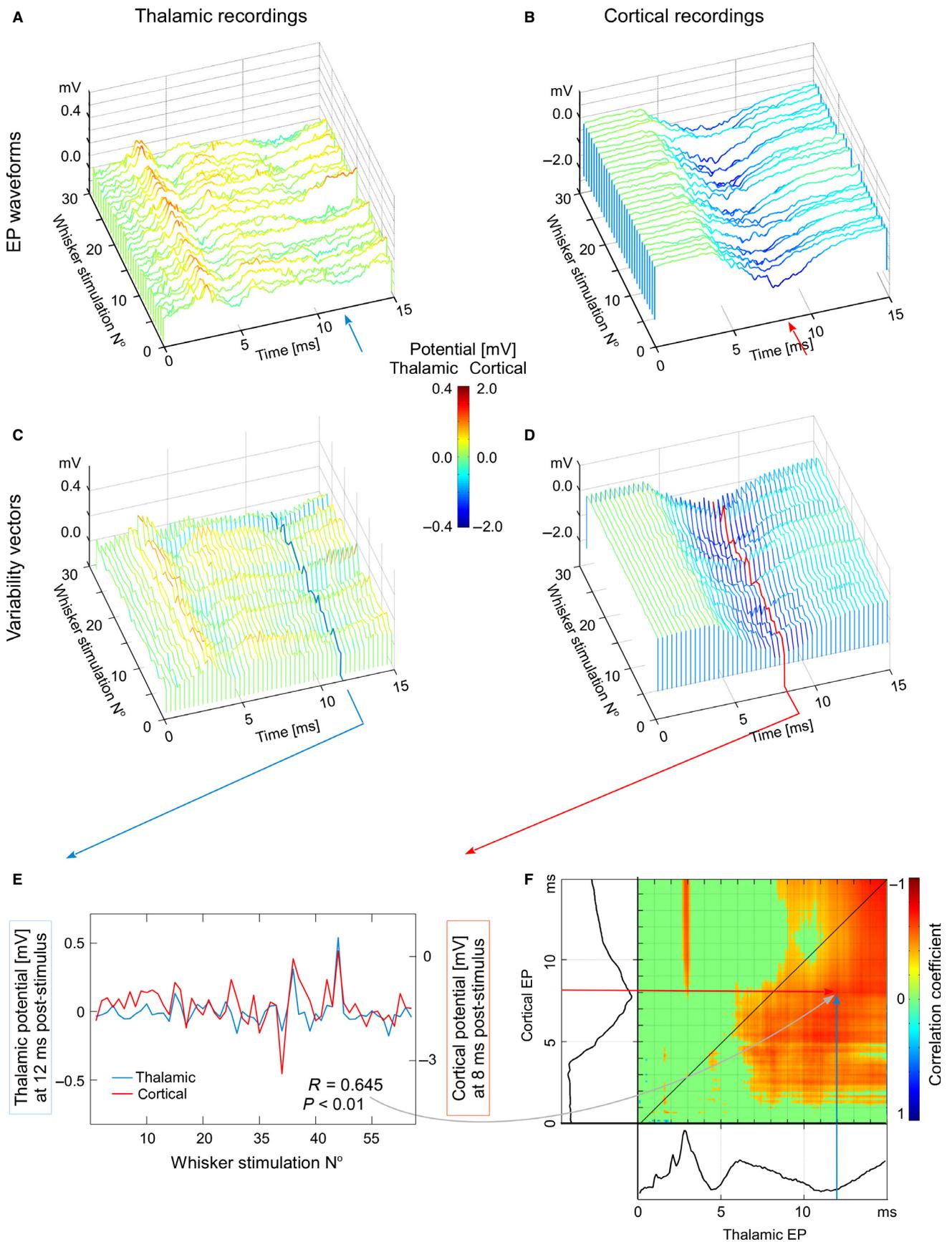Thalamic   Cortical

E

F

$R = 0.645$
$P < 0.01$

FIG. 2. Cross-trial-correlation (CTC) method. (A–D) Example of 30 single responses evoked by consecutive whisker stimulations in thalamic (A, C) and cortical (B, D) electrodes during one recording session in awake aroused condition. In the upper row (A, B) lines are drawn along EP waveforms; in the lower row (C, D) lines connect points of the same latency from consecutive trials emphasizing trial-to-trial variability of consecutive EP time samples (10 kHz sampling rate, for clarity we draw every third sample). Single lines are outlined at 12 ms post-stimulus in thalamic recording (C) and at 8 ms post-stimulus in cortical recording (D) and then overlaid in E. (E) The left axis indicates scale for thalamic, and right axis for cortical values of potentials. Single run of CTC correlates a pair of variability vectors from two sites. The resulting correlation coefficient value (R) for an example pair in E is plotted in the CTC correlation matrix (F) at the crossing of the two latencies (12 ms in thalamus and 8 ms in cortex). The analysis is repeated for all combinations of thalamic and cortical post-stimulus latencies and the correlation matrix is filled with corresponding coefficient values. Non-significant (a two-dimensional implementation of a cluster-based permutation test, see Methods) coefficients are substituted by zero and plotted in green (light grey in print). (F) CTC correlation matrix calculated for 60 EPs from this session (average EP waveforms plotted on the sides of the matrix). A high correlation value – reflecting strong functional connection – is achieved when variability in one structure at a particular latency predicts variability in the other structure at a longer latency.

coefficient r are calculated by transforming the correlation coefficient into its corresponding t-statistic using the formula $t = r/\sqrt{((1 - r^2)/(n-2))}$, where n is the sample size used to calculate r, and obtaining the P-value from Student's t distribution for $n-2$ degrees of freedom.

(3) All surviving adjacent elements are clustered (an element is considered adjacent if it has a non-zero neighbour to the left, to the right, above or below it in the matrix) and the weight of the most massive cluster (i.e. the sum of the absolute values of correlation coefficients constituting the cluster) is recorded.

(4) Steps 1–3 are repeated 500 times and an empirical distribution is built from the most massive randomly created clusters from each permutation.

(5) From the original (uncorrected) CTC matrix we removed (substituted with zeros) all clusters whose weights were greater than the first and less than the 99th percentile (essentially equivalent to $P > 0.01$).

Long-range field effects in LFP data

The extent to which LFP signal propagates from the source of its generation is reported to range from several millimetres (Kreiman *et al.*, 2006) to < 250 μm (Katzner *et al.*, 2009; Xing *et al.*, 2009). As vibrissal representations in VPM and PoM are adjacent and have centres that are ~500 μm apart (Paxinos & Watson, 2007), interference of their activity evoked by potent multiwhisker stimulation can be expected in recorded signals. Consequently, CTC matrices calculated from such mixed signals express summed not individual interactions of the cortex with both somatosensory nuclei. To control for such possible interference, we developed an algorithm that eliminates those elements of the correlation matrices that are most likely to be passive 'echoes' of activity generated in neighbouring structures.

In the following description, PoM, VPM and barrel cortex are denoted as X, Y and Z. X and Y are anatomically adjacent and both receive sensory driving input; subsequently, they both drive a distant structure Z. CTC analysis for X–Z and Y–Z generates two correlation matrices (M_{XZ} and M_{YZ}) each containing t^2 elements (correlations coefficients), where t is the number of samples in the EP epochs used (here: 250). Let us denote each of those elements as $r_{XZ}(i,j)$ or $r_{YZ}(i,j)$, respectively, where $i, j = 1, 2, \ldots, 250$. We now describe the procedure for the field effect correction below:

(1) We re-calculate CTC matrices a large number of times (here: 500), but in each permutation using EPs only from a random sample of trials (here: $n = 100$; a jack-knife-type procedure).

(2) Consequently, each element of the original M_{XZ} matrix can now be assigned a corresponding 500-element vector (let us call it '$V_{XZ}(i,j)$') of correlation coefficients generated in the jack-knife procedure. Similarly, each element of the original matrix M_{YZ} now can be assigned a 500-element vector '$V_{YZ}(i,j)$'.

(3) For every (i,j) pair we calculate a correlation coefficient between vector $V_{XZ}(i,j)$ and its counterpart $V_{YZ}(i,j)$. Let us denote those coefficients as $R(i,j)$. Those elements of both original matrices R_{XZ} and R_{YZ} for which there was a clear correlation between vectors V_{XZ} and V_{YZ} (here: $R > 0.6$) are considered to reflect field effects generated by local processes in one of the structures that show-up as crosstalk in the neighbouring structure. As the strength of activity is greater when closer to its source, the source belongs to that of the original M_{XZ} and M_{XZ} matrices in which the given element is larger. The corresponding element in the other matrix is considered to be an 'echo' attributable to the crosstalk, and removed (substituted with a zero). Of course X and Y (PoM and VPM) might be active exactly at the same time and both can influence Z (cortex) with different strength. After 'field-effect' correction only the stronger connection would be preserved in the CTC matrix. Thus, when interpreting the results we look at the relative but not absolute strengths of PoM and VPM inputs to the cortex.

Analysis of behaviour

During each session in which the animals were awake we observed them to control the level of habituation to the experimental situation (we judged the amount of audible vocalization, large body movements, urination and defecation). The rats' spontaneous behaviour and behavioural reactions to whisker stimulation were also quantified off-line by image analysis of the video files that were recorded during sessions. Because the image background was stationary, any changes between consecutive video frames can be attributed solely to the movements of the rat's snout. For the quantitative analysis video files were imported to the Matlab environment. Each digitized frame is an $x \times y \times z$ array of integers from 0 to 255. By performing an element-wise subtraction of each frame from its successor followed by a summation of the absolute values of the resultant differences, we obtained a train of numbers that are synchronous with the electrophysiological signal and that quantify the global changes on the screen (i.e. amount of rat's motion). We analysed the motion values in the 400-ms window before the whisker stimulus (spontaneous, pre-stimulus motion) and in the corresponding 400-ms window after the stimulus (post-stimulus motion). Each rat's reactions to whisker stimulation were estimated by comparing the maximal values from these epochs before and after the stimulus (Fig. 3A).

Results

Arousal level

To investigate the arousal-related reorganization of the thalamo-cortical somatosensory routes, we recorded EPs from the barrel cortex, VPM and PoM in the same group of rats at three vigilance levels: anaesthetized, quiescent wakefulness and highly aroused (alarmed) wakefulness. The level of arousal in awake animals was manipulated first via the long-lasting habituation to experimental conditions (depending on an individual anxiety level, a rat would need 4–8

A Single-trial behavioral response

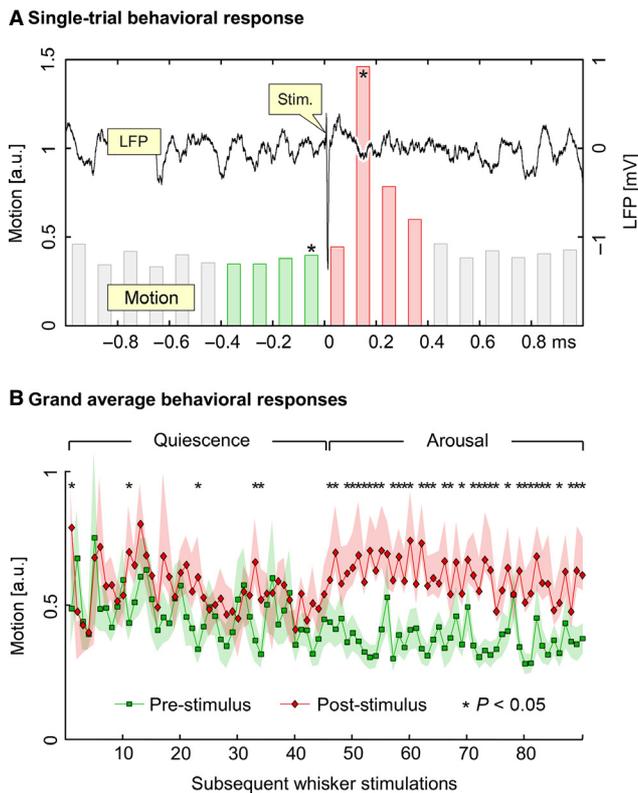**B** Grand average behavioral responses

FIG. 3. The rats' behavioural reactions to whisker stimulation (see Methods) quantified by image analysis of the video files. (A) Example of a rat's reactions to whisker stimulation (bars) presented along a single LFP sweep. Each rat's reactions to whisker stimulation were estimated by comparing maximum 'motion' values (indicated by asterisks) that were obtained during 400 ms before the stimulus (applied at time 0 in A) with the corresponding values that were obtained during 400 ms after the stimulus. (B) Data pairs from all sessions and all rats in which the animal was awake were aligned based on the first aversive stimulation and compared using a paired *t*-test (asterisks denote differences significant at $P < 0.05$). Note increased reaction (i.e. increased difference between pre- and post-stimulus motion level) during the arousal session.

sessions to become quiescent) and then by an application of additional aversive stimuli. A stable level of habituation was accompanied by disappearance of audible vocalization; large body movements (fighting against the hammock) were replaced by infrequent small position corrections; there was neither urination nor defecation during the session; online observation of recorded LFPs indicated a large incidence of idling oscillations at 5–12 Hz (Sobolewski *et al.*, 2011). The arousing effect of aversive stimuli was confirmed in our previous experiments by very strong and reliable LFP spectrum desynchronization (Musiał *et al.*, 1998; Sobolewski *et al.*, 2011) which we could also observe online as a reduced incidence of 5–12 Hz oscillations. Here, as shown by video analysis, we also observed behavioural changes: a decrease of spontaneous mobility (freezing) and increased intensity of the rat's behavioural ('startle') reactions to the whisker stimuli (Fig. 3B). Other behavioural evidence of aversive agitation was reappearance of droppings in the hammock after arousal sessions.

Somatosensory evoked potentials

Examples of four consecutive EPs that were recorded from one animal in a state of wakeful quiescence are shown in Fig. 4A–C. Although the stimulus was identical for each recording, the EPs showed a degree

of variability that is typical for single-trial sensory responses (Figs 2 and 4A–C). It is now widely accepted that such variability results to a large extent from the momentary state of the network that is involved in stimulus processing (Arieli *et al.*, 1996; Renart & Machens, 2014). We take advantage of this variability to assess functional connectivity between cerebral structures, which is described below as the main result of this paper. However, to extract reproducible response features that are typical for the tested locations and experimental conditions, we also analysed responses at the different vigilance levels with a conventional averaging approach.

The average EP that was recorded from VPM consisted of a negative wave (N1.1 in Fig. 4D) that represented a net excitation (aggregated postsynaptic potentials; PSPs) from sensory afferents (Kublik *et al.*, 2003). Conversely, in PoM, the first wave was positive (P1 in Fig. 4E), which was most likely attributable to early feed-forward inhibitory input from the zona incerta (Lavallée *et al.*, 2005). Although this pattern was consistent across all of the arousal states that we tested, the dynamics of these initial responses changed as a result of the transition from anaesthetized state to wakefulness: the peak latency of N1.1 in VPM shortened (by 0.5 ms), and its amplitude increased by 24%, whereas the amplitude of P1 in PoM decreased by 35% (these and all the following quoted amplitude changes were confirmed to be statistically significant at $P < 0.05$ as determined by a Student's *t*-test; Fig. 4D and E). Furthermore, during wakefulness, the peripheral input evoked the synchronized discharge of thalamic cells; this discharge was reflected in a biphasic population spike (Fig. 4D and E) that was superimposed on the compound PSP components. We believe that this prominent component recorded in awake rats reflects population spike activity evoked by strong, well-synchronized multi-whisker input, as its latency corresponds to that observed in single-cell recordings in VPM (Diamond *et al.*, 1992b) and PoM (Ahissar *et al.*, 2000) and is further seen as an incoming volley at the earliest phase of cortical evoked potential (Fig. 4F; see below). This wave recorded in PoM had slightly shorter latency (5 ms) than onset of spike responses reported by Ahissar *et al.* (2000) (6 ms), which might be related to different methods of stimulation of whiskers used in the two studies: direct touch delivered by a piezoelectric stimulator versus 50-ms air puff used by Ahissar *et al.* (2000). The amplitude of this spike increased during the transition from a state of quiescent wakefulness to one of high arousal (see significance bars in Fig. 4D and E). Subsequent thalamic EP waves (N1.2 and P2 in Fig. 4D and E) mostly reflected aggregated PSPs dependent on recurrent cortical influence (we have previously shown that these waves disappear after suppression of the cortex; Kublik *et al.*, 2003). The dynamics of these waves also changed with changes in arousal state: they were barely discernible during anaesthesia, they were present during quiescence and they had increased amplitudes during states of high arousal.

The cortical response (Fig. 4F), which was recorded from layer 5 of barrel cortex during wakefulness, commences with an incoming sensory volley that corresponds to the thalamic population spike (Kublik *et al.*, 2001) visible in the cortex with 0.6-ms delay. This activity is then followed by the negative N1 wave, which is mainly generated by PSPs from cortical pyramidal cells (Wróbel *et al.*, 1998; Kublik *et al.*, 2001). During anaesthesia, the incoming volley cannot be distinguished from N1, the amplitude of which is significantly smaller than it is in other states of vigilance.

CTC analysis

Conventional analysis of averaged EPs does not provide direct information about inter-structure connectivity, nor is it possible to make

Single-trial EP examples:

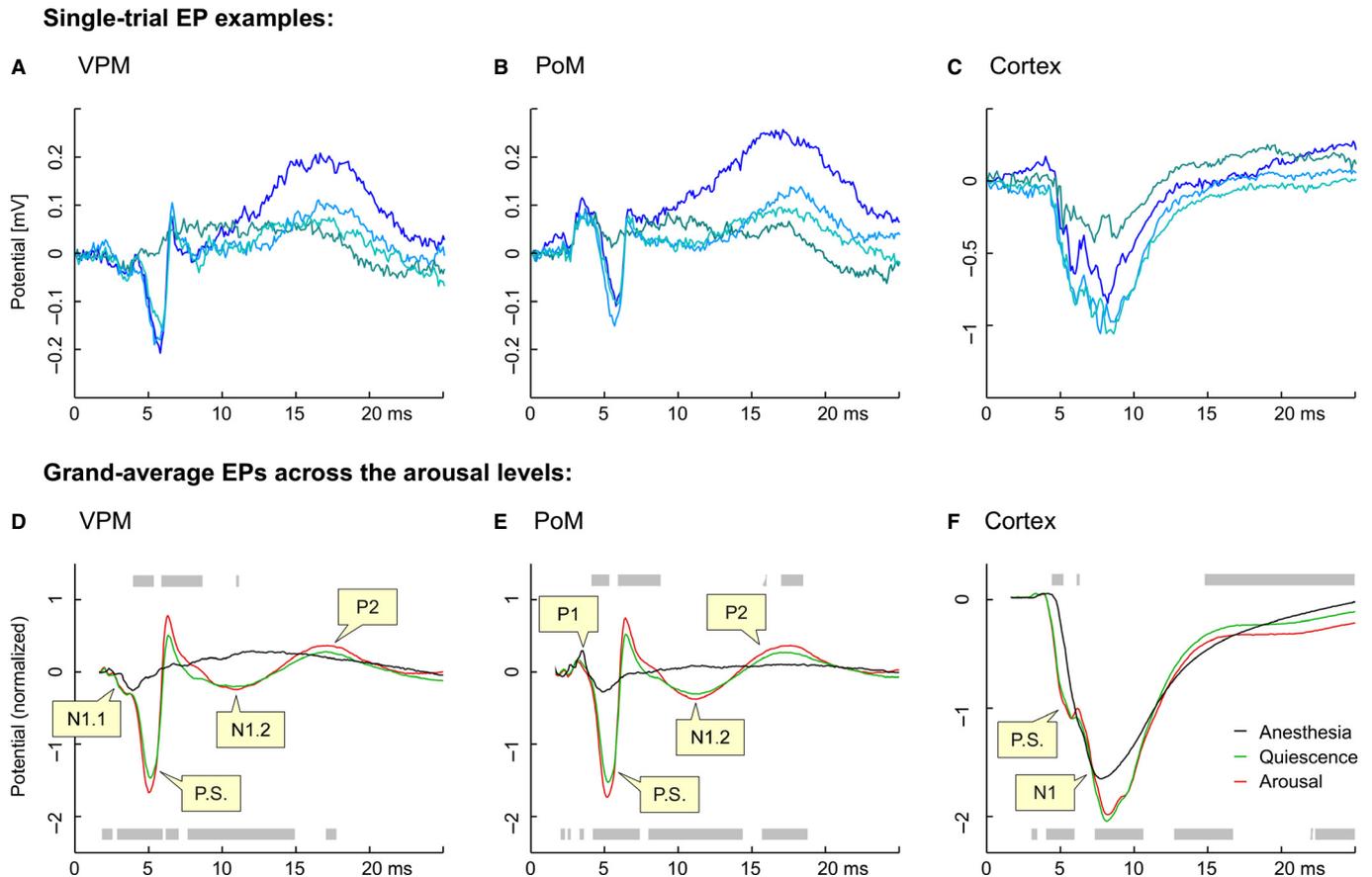**Grand-average EPs across the arousal levels:**

FIG. 4. (A–C) Examples of single-trial EPs (four consecutive trials randomly picked from the dataset of 800) recorded from the thalamus (A, VPM; B, PoM nuclei) and the primary somatosensory cortex (layer 5 of the barrel field, C) of one rat during quiescent wakefulness. The large amplitude difference between thalamic and cortical recordings stems from their different cellular components – the geometry of cortical pyramidal cells is responsible for strong open field electric dipoles while thalamic cells generate much weaker, partially closed electric fields. (D–F) Grand averages of EPs recorded from the VPM (D), PoM (E) and the barrel field (F) of rats ($n = 5$) across three behavioural states: anaesthesia, quiescent wakefulness and high arousal. Grey segments below the traces indicate the latencies at which anaesthetized and quiescent EPs differ significantly (*t*-test, $P < 0.05$). The grey segments above the traces indicate the latencies at which high-arousal and quiescent EPs differ significantly (*t*-test, $P < 0.05$). (D, E) N1.1 – initial thalamic excitation from sensory afferents which for PoM is preceded by a small positive wave (P1) probably attributable to rapid feed-forward inhibitory input from the zona incerta and/or anterior pretectal nucleus. P.S. – population spike visible in awake conditions; N1.2 and later P2 – respectively excitatory and inhibitory responses largely dependent on cortical influences (Kublik *et al.*, 2003). (F) P.S. – population spike from thalamus arriving to the cortex through thalamo-cortical fibres; N1 – main cortical wave built up pyramidal cell's postsynaptic activity (Kublik *et al.*, 2001).

such inferences from single EPs. To extract connectivity information we have applied the CTC method, which assesses the coupling strengths between different cerebral sites based on the co-variance of their various EP components. The results of CTC are visualized as correlation matrices in which clusters of significant coefficients link the features of EPs from different sites. This in turn reveals the strengths and temporal patterns of the functional connections between these sites during the processing of sensory stimuli (Figs 2 and 5).

When CTC was applied in this experiment, the EPs that were recorded during anaesthesia revealed only the FO sensory activation of the cortex, which was demonstrated by a cluster of correlations in VPM–cortex matrix (Fig. 5A). No significant correlations were found between other sites of the thalamo-cortical system when the animals were in this state.

During quiescent wakefulness, the well-synchronized VPM response, which peaked 5 ms following stimulus with the population spike, drove the main cortical EP wave (N1). This coupling is visualized in Fig. 5B as correlation cluster 1a; subsequent thalamocortical activity of VPM at later latencies (Diamond *et al.*, 1992b) seems to be represented by cluster 2. A striking qualitative change from anaesthesia includes the appearance of a recurrent flow to the thala-

mus (attributed mainly to PoM – right side of Fig. 5B, not VPM – left side of this figure) that follows in time the main cortical N1 response. This can be seen from the correlation clusters (labelled 3 and 4 in Fig. 5B) that appeared below the diagonal in the cortex–PoM matrix.

Colours of the clusters indicate unidirectional (red) and opposite direction (blue) changes of potential amplitude. For physiological interpretation one needs to consider also the polarity of EP deflections. Cluster 1 links the negative phase of the population spike with negative cortical N1 wave – red colour indicates that increased amplitude of the population spike (stronger thalamic response) is followed by larger amplitude of N1 (stronger activation of cortical pyramids). Blue cluster 4 links cortical N1 with thalamic P2. Stronger cortical activity represented by deeper N1 is accompanied by more positive P2 – most probably indirect inhibition initiated from the cortex and reaching the thalamus through reticular nucleus of the thalamus and/or ZI or APT.

The functional thalamo-cortical network was further rearranged when the animal's arousal level was increased by the introduction of aversive stimuli (Fig. 5C). First, the strength of the input from VPM to barrel cortex diminished, which is represented by the weaker
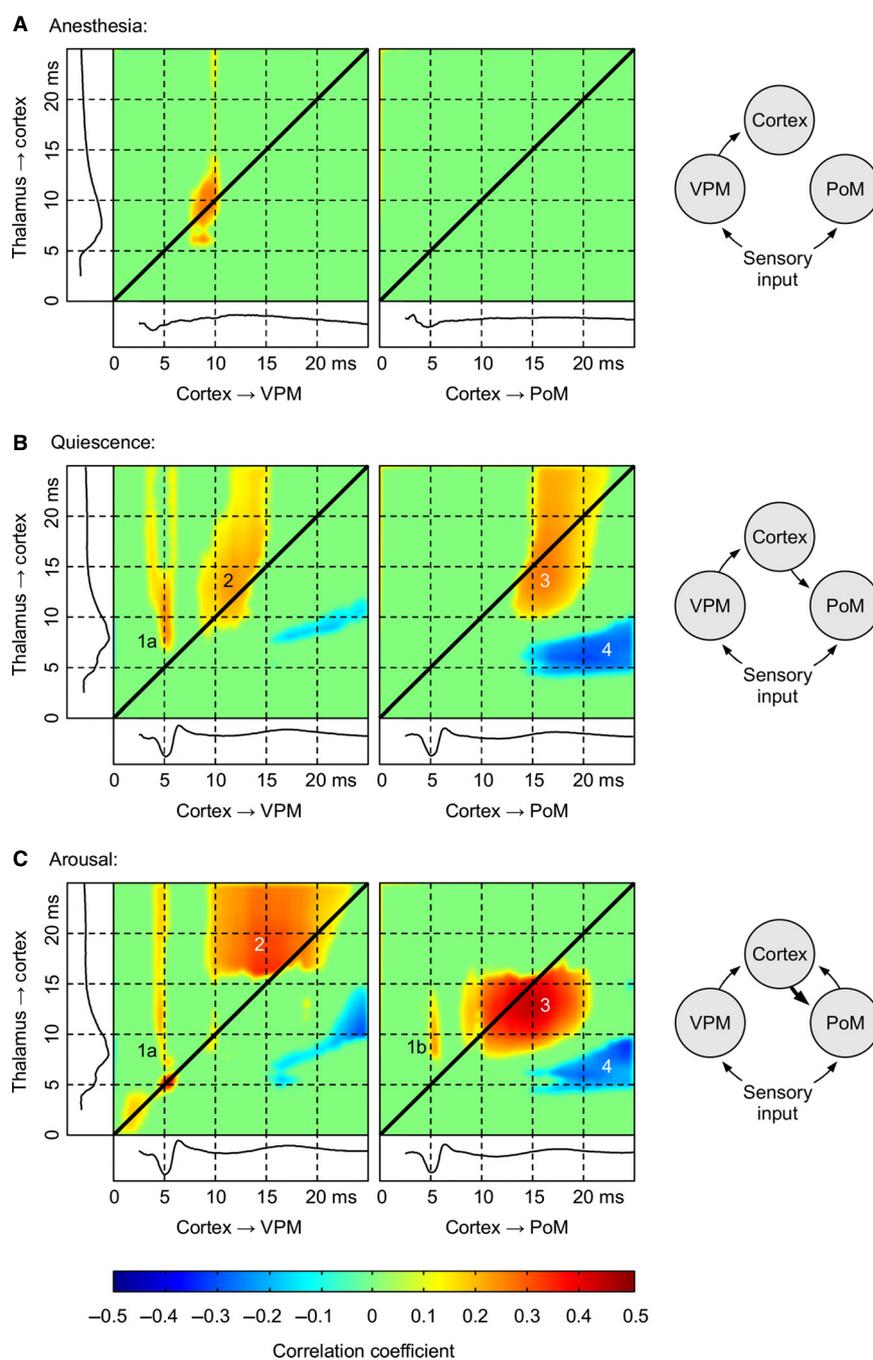
FIG. 5. Functional connectivity assessed using cross-trial correlation (CTC) between first-order thalamic nuclei (VPMs), higher-order thalamic nuclei (PoMs) and the primary somatosensory cortex (layer 5 of the barrel field) of five rats during sensory processing in three behavioural states: (A) anaesthesia, (B) quiescent wakefulness and (C) high arousal. CTC reveals the relationships between single EPs recorded at different levels of the sensory processing. The results are visualized as a correlation matrix; the average EPs from the correlated sites are plotted below the matrix and to the left of it for temporal reference. Coloured blobs, i.e. clusters of significant correlation coefficients ($P \leq 0.01$ in two-dimensional cluster-based permutation test, see Methods) that appear in the matrix link features of the EPs that were recorded simultaneously from the two sites and reveal the strengths and temporal patterns of the functional connections between them. Colours of the clusters indicate unidirectional (positive correlation, red, clusters 1, 2 and 3) and opposite direction (negative correlation, blue, cluster 4) changes of potential amplitude. For example, the red colour of cluster 1 (in B and C) indicates that increased amplitude of a thalamic population spike (stronger thalamic response) is followed by larger amplitude of N1 (stronger activation of cortical pyramids). Blue cluster 4 links cortical N1 with thalamic P2: more negative cortical N1 is accompanied by more positive P2 – most probably illustrating indirect inhibition initiated from the cortex and reaching the thalamus through reticular nucleus of the thalamus and/or ZI or APT. Darker (red or blue) clusters indicate more efficient (stronger) connections; paler (greenish or yellowish) clusters suggest weaker connections (the values of the correlation coefficients can be determined from the colour bar at the bottom of the figure). Transmission delays cause the clusters to appear to be shifted either above or below the main diagonals of the matrices, which thereby implicates a directional effect. When EP waves are separated by short time delays and overlap in time they generate clusters embracing the diagonal (e.g. cluster 3). In such cases the location of the larger part of a cluster together with its maximal values indicate dominant transfer direction (a strictly simultaneous phenomenon would yield clustering precisely on the diagonal). See Methods and our previous methodological paper (Sobolewski *et al.*, 2010) for a full explanation of the algorithms. Schematic drawings to the right of the CTC matrices provide graphical interpretations of the results that are contained in the matrices. The thicker arrow denotes the connection for which there is an increase in functional strength during high arousal. The results depicted represent aggregate results for the same animals as in Fig. 4D–F.

correlation cluster labelled 1a (left panel). Concurrently, however, the strength of the early connection from PoM to barrel cortex increased, which is manifested as the appearance of correlation cluster 1b in Fig. 5C (right panel). The recurrent cortico-thalamic connections to PoM were also strengthened (compare the values of the coefficients in cluster 3 in Fig. 5B and C).

Discussion

Our results show that a description of thalamic connectivity which defines PoM as the HO relay, as opposed to the FO VPM (Reichova & Sherman, 2004; Theyel *et al.*, 2010), should be elaborated to account for dynamic, state-dependent network reconfiguration: at a low level of arousal, the sensory signal is indeed primarily relayed by VPM to the barrel cortex and then from the cortex to PoM. However, at a high level of arousal, this network is short-circuited, and the cortex also receives fast sensory input directly via PoM (Fig. 5C, cluster 1b and diagram to the right). Therefore, instead of being described as the HO relay, PoM should be regarded as the mixed-type relay because it is capable of operating in either HO or FO mode. Such a possibility has been proposed by Sherman (2001), and suggested by convergence of subcortical and cortical driving inputs on individual thalamic neurons (Groh *et al.*, 2014) but until now there has been no functional *in vivo* data to either support or discount this hypothesis.

Our conclusion was possible due to application of CTC analysis to tactile evoked potentials recorded from both anaesthetized and drug-free animals, which demonstrated how the flow of information within the thalamo-cortical loops varies with an animal's level of arousal. During anaesthesia, the only cluster of correlation appeared in the VPM–cortex matrix (Fig. 5A) and it can be attributed to the FO pathway because it corresponds to short-latency activation of VPM at approximately 7 ms after the tactile stimulus (Diamond *et al.*, 1992b; Kublik *et al.*, 2003) and has a temporal range allowing for early cortical responses (N1) of approximately 7–15 ms following stimulus (Armstrong-James *et al.*, 1992; Shimegi *et al.*, 1999; Kublik *et al.*, 2003). The lack of any significant correlations between PoM and cortical LFP responses in anaesthetized animals corresponds to the scattered activation of PoM neurons during urethane anaesthesia (Diamond *et al.*, 1992b); this activation is too weak and temporally dispersed to evoke a synchronized cortical postsynaptic response. We were also unable to observe feedback responses in the thalamus, which agrees with the observation that activity in cortical infragranular layers, where cortico-thalamic neurons reside, is suppressed during anaesthesia (Armstrong-James & George, 1988). Only when the animals were awake did we observe cortico-thalamic feedback activation in the CTC matrix, and that activation was principally directed to PoM (cluster 3 in Fig. 5B). This result can be explained by the driving influence of cortical layer 5b over PoM and lack of that influence in VPM, which receives only modulatory cortical input from layer 6 (Veinante *et al.*, 2000). We assume that the observed cortico-thalamic influence comes from the barrel cortex from which we have recorded and for which CTC detected significant correlation. This conclusion corroborates an earlier report showing that action potentials in PoM neurons can be triggered from layer 5 of the barrel cortex with latencies of approximately 7 ms (Groh *et al.*, 2014). Of course other cortical areas could also participate in such top-down information flow. Involvement of the secondary somatosensory cortex (S2) is possible as it sends both layer 6 and 5 axons to PoM (Lévesque *et al.*, 1996). Primary motor cortex (M1) was shown to modulate PoM activity, although this effect was observed during active whisking (Urbain & Deschênes, 2007) in the periods before the whisker–stimulus contact

was made (Pais-Vieira *et al.*, 2013). With passive detection of unexpected stimuli, a role of the motor cortex is less likely, especially as cortical motor neurons respond to mechanical whisker stimulation at longer latencies than the barrel cortex (Chakrabarti *et al.*, 2008), too late to influence PoM activity at 13–20 ms after stimulus.

An explanation of the effects observed during high arousal, notably the takeover of a significant portion of the thalamo-cortical traffic by PoM, requires further discussion. We have previously shown (Sobolewski *et al.*, 2010), and replicate here (Fig. 5B and C), that the transfer of sensory information through the first-order VPM in awake rats is attenuated by increases in arousal, which is most probably due to the neuromodulatory retuning of thalamo-cortical functional connectivity. This result corroborates earlier observations (Castro-Alamancos & Oldford, 2002) and is best explained by the frequency-dependent depression of VPM–cortical synapses, which results from the rise in thalamic tonic firing during arousal (Castro-Alamancos & Oldford, 2002). On the other hand, frequency-dependent depression has not been found in inputs from PoM to cortical layer 5a (Castro-Alamancos & Connors, 1997; Viaene *et al.*, 2011), which means that during arousal cortical input from PoM can increase in strength relative to input from VPM.

Another physiological mechanism explaining our results links the state-dependent gating of flow of sensory information via PoM with its inhibition by ZI. Trageser & Keller (2004) showed that in anaesthetized rats, after lesioning ZI PoM responds to peripheral input with short latencies, in a manner similar to that of FO relays. Because ZI provides feed-forward GABAergic inhibition to PoM and other thalamic nuclei regarded as HO relays (Power *et al.*, 1999, 2001; Barthó *et al.*, 2002), it was proposed that ZI operates a gating mechanism that regulates this route to the cortex (Trageser & Keller, 2004).

Experiments in anaesthetized animals showed that activity of ZI neurons is prone to arousal-related neuromodulation, as pharmacological or electric brainstem cholinergic activation results in inhibition of GABAergic projection neurons in ZI (Masri *et al.*, 2006; Trageser *et al.*, 2006). ZI could also be inhibited by APT nucleus, known to be involved in stress and pain-related sensory transmission (Murray *et al.*, 2010). Therefore, at low arousal levels, inhibition from ZI would prohibit the flow of ascending sensory information through PoM, enabling a greater flow of information with increasing arousal. Our findings are fully consistent with the hypothesis of brain state-dependent regulation of the transfer of sensory information in PoM by ZI/APT. Not only have we provided evidence for the functional reorganization of the thalamo-cortical network in different behavioural states, but also observed LFP changes indicating a direct influence of the ascending inhibitory pathways on PoM. Because we recorded continuously when an animal demonstrated different levels of arousal, we confirmed that the initial positive wave of evoked potentials in PoM (P1 in Fig. 2E), which we attribute to the feed-forward inhibitory input, was pronounced in the anaesthetized state. In awake animals, this wave was significantly smaller and was followed by a population spike that demonstrated an early, synchronized response in PoM cells.

It should be added that our results do not contradict another hypothesis, proposed by Lavallée *et al.* (2005), which states that incertal GABAergic cells that project to PoM could be inhibited directly by intra-incertal connections and through them by collaterals of fibres that descend from cortical layer 5b and carry motor instructions to PoM and the brainstem motor centres. In this scenario, incertal inhibition of PoM would be reduced during active vibrissal exploration with whisking movements (Lavallée *et al.*, 2005), allowing for convergence of peripheral and cortical inputs in PoM (Groh

et al., 2014). This mechanism would provide an 'AND-gate' comparator for intended and actual whisking (Ahissar & Oram, 2015). Such a situation was beyond the scope of our experiment because we applied only passive vibrissal stimuli. However, we propose that the two gating mechanisms (whisking-related and arousal-related) are not mutually exclusive. During anaesthesia, when the sensory systems are not sensitive to contextual demands, and when cortical motor commands are absent, HO circuits do not operate (as we observed in the case of the somatosensory PoM nucleus). During quiescent wakefulness when an animal explores its environment, motor (whisking) commands from the cortex are sent to ZI (to reduce its activity and thus disinhibit PoM) and to PoM for comparison with peripheral whisking-related tactile signals (the 'comparator' mode of PoM activity). In the more vigilant state (e.g. related to stressful context as in our experiment) it is cholinergic neuromodulation that reduces ZI activity and shifts mixed-type relays such as PoM toward an FO 'detector mode'. PoM working in the 'detector mode' would serve to supply the primary somatosensory cortex with information on context-dependent saliency of tactile stimuli. Another consequence of functional reorganization in response to changes in arousal may be even more significant. Because PoM is also directly connected to higher sensory and motor cortices (Ohno *et al.*, 2012), a shortcut that is unlocked when an animal is alarmed may serve to facilitate a behavioural reaction during fear-related arousal at the justifiable expense of accurately processing stimulus features (PoM receptive fields are less precise than VPM receptive fields; Williams *et al.*, 1994). In an ethological sense, this could be stated as: if alarmed when encountering a stimulus, even if it was previously known to be neutral, run first, and analyse later.

Acknowledgements

Abbreviations

APT, anterior pretectal nucleus; CTC, cross-trial-correlation; EP, evoked potential; EPSP, excitatory postsynaptic potential; FO, first-order thalamic nuclei; HO, higher order thalamic nuclei; LFP, local field potential; PoM, postero-medial nucleus; VPM, ventral postero-medial nucleus; ZI, zona incerta.

References

Aertsen, A.M., Gerstein, G.L., Habib, M.K. & Palm, G. (1989) Dynamics of neuronal firing correlation: modulation of 'effective connectivity'. *J. Neurophysiol.*, **61**, 900–917.

Ahissar, E. & Oram, T. (2015) Thalamic relay or cortico-thalamic processing? Old question, new answers. *Cereb. Cortex*, **25**, 845–848.

Ahissar, E., Sosnik, R. & Haidarliu, S. (2000) Transformation from temporal to rate coding in a somatosensory thalamocortical pathway. *Nature*, **406**, 302–306.

Arieli, A., Sterkin, A., Grinvald, A. & Aertsen, A. (1996) Dynamics of ongoing activity: explanation of the large variability in evoked cortical responses. *Science*, **273**, 1868–1871.

Armstrong-James, M. & George, M.J. (1988) Influence of anesthesia on spontaneous activity and receptive field size of single units in rat Sm1 neocortex. *Exp. Neurol.*, **99**, 369–387.

Armstrong-James, M., Fox, K. & Das-Gupta, A. (1992) Flow of excitation within rat barrel cortex on striking a single vibrissa. *J. Neurophysiol.*, **68**, 1345–1358.

Barthó, P., Freund, T.F. & Acsády, L. (2002) Selective GABAergic innervation of thalamic nuclei from zona incerta. *Eur. J. Neurosci.*, **16**, 999–1014.

Bokor, H., Frère, S.G.A., Eyre, M.D., Slézia, A., Ulbert, I., Lüthi, A. & Acsády, L. (2005) Selective GABAergic control of higher-order thalamic relays. *Neuron*, **45**, 929–940.

Castro-Alamancos, M.A. & Connors, B.W. (1997) Thalamocortical synapses. *Prog. Neurobiol.*, **51**, 581–606.

Castro-Alamancos, M.A. & Oldford, E. (2002) Cortical sensory suppression during arousal is due to the activity-dependent depression of thalamocortical synapses. *J. Physiol.*, **541**, 319–331.

Chakrabarti, S., Zhang, M. & Alloway, K.D. (2008) MI neuronal responses to peripheral whisker stimulation: relationship to neuronal activity in SI barrels and septa. *J. Neurophysiol.*, **100**, 50–63.

Diamond, M.E., Armstrong-James, M., Budway, M.J. & Ebner, F.F. (1992a) Somatic sensory responses in the rostral sector of the posterior group (POm) and in the ventral posterior medial nucleus (VPM) of the rat thalamus: dependence on the barrel field cortex. *J. Comp. Neurol.*, **319**, 66–84.

Diamond, M.E., Armstrong-James, M. & Ebner, F.F. (1992b) Somatic sensory responses in the rostral sector of the posterior group (POm) and in the ventral posterior medial nucleus (VPM) of the rat thalamus. *J. Comp. Neurol.*, **318**, 462–476.

Einevoll, G.T., Kayser, C., Logothetis, N.K. & Panzeri, S. (2013) Modelling and analysis of local field potentials for studying the function of cortical circuits. *Nat. Rev. Neurosci.*, **14**, 770–785.

Groh, A., Bokor, H., Mease, R.A., Plattner, V.M., Hangya, B., Stroh, A., Deschenes, M. & Acsády, L. (2014) Convergence of cortical and sensory driver inputs on single thalamocortical cells. *Cereb. Cortex*, **24**, 3167–3179.

Hoogland, P.V., Wouterlood, F.G., Welker, E. & der Loos, H.V. (1991) Ultrastructure of giant and small thalamic terminals of cortical origin: a study of the projections from the barrel cortex in mice using *Phaseolus vulgaris* leuco-agglutinin (PHA-L). *Exp. Brain Res.*, **87**, 159–172.

Katzner, S., Nauhaus, I., Benucci, A., Bonin, V., Ringach, D.L. & Carandini, M. (2009) Local origin of field potentials in visual cortex. *Neuron*, **61**, 35–41.

Korzeniewska, A., Crainiceanu, C.M., Kuś, R., Franaszczuk, P.J. & Crone, N.E. (2008) Dynamics of event-related causality in brain electrical activity. *Hum. Brain Mapp.*, **29**, 1170–1192.

Kreiman, G., Hung, C.P., Kraskov, A., Quiroga, R.Q., Poggio, T. & DiCarlo, J.J. (2006) Object selectivity of local field potentials and spikes in the macaque inferior temporal cortex. *Neuron*, **49**, 433–445.

Kublik, E., Musiał, P. & Wróbel, A. (2001) Identification of principal components in cortical evoked potentials by brief surface cooling. *Clin. Neurophysiol.*, **112**, 1720–1725.

Kublik, E., Swiejkowski, D.A. & Wróbel, A. (2003) Cortical contribution to sensory volleys recorded at thalamic nuclei of lemniscal and paralemniscal pathways. *Acta Neurobiol. Exp.*, **63**, 377–382.

Lavallée, P., Urbain, N., Dufresne, C., Bokor, H., Acsády, L. & Deschênes, M. (2005) Feedforward inhibitory control of sensory information in higher-order thalamic nuclei. *J. Neurosci.*, **25**, 7489–7498.

Lévesque, M., Gagnon, S., Parent, A. & Deschênes, M. (1996) Axonal arborizations of corticostriatal and corticothalamic fibers arising from the second somatosensory area in the rat. *Cereb. Cortex*, **6**, 759–770.

Maris, E. & Oostenveld, R. (2007) Nonparametric statistical testing of EEG- and MEG-data. *J. Neurosci. Meth.*, **164**, 177–190.

Masri, R., Trageser, J.C., Bezdudnaya, T., Li, Y. & Keller, A. (2006) Cholinergic regulation of the posterior medial thalamic nucleus. *J. Neurophysiol.*, **96**, 2265–2273.

Murray, P.D., Masri, R. & Keller, A. (2010) Abnormal anterior pretectal nucleus activity contributes to central pain syndrome. *J. Neurophysiol.*, **103**, 3044–3053.

Musiał, P., Kublik, E., Panecki, S.J. & Wróbel, A. (1998) Transient changes of electrical activity in the rat barrel cortex during conditioning. *Brain Res.*, **786**, 1–10.

Ohno, S., Kuramoto, E., Furuta, T., Hioki, H., Tanaka, Y.R., Fujiyama, F., Sonomura, T., Uemura, M., Sugiyama, K. & Kaneko, T. (2012) A morphological analysis of thalamocortical axon fibers of rat posterior thalamic nuclei: a single neuron tracing study with viral vectors. *Cereb. Cortex*, **22**, 2840–2857.

Pais-Vieira, M., Lebedev, M.A., Wiest, M.C. & Nicolelis, M.A.L. (2013) Simultaneous top-down modulation of the primary somatosensory cortex and thalamic nuclei during active tactile discrimination. *J. Neurosci.*, **33**, 4076–4093.

Paxinos, G. & Watson, C. (2007) *The Rat Brain in Stereotaxic Coordinates*, 6th Edn. Academic Press, New York.

Power, B.D., Kolmac, C.I. & Mitrofanis, J. (1999) Evidence for a large projection from the zona incerta to the dorsal thalamus. *J. Comp. Neurol.*, **404**, 554–565.

Power, B.D., Leamey, C.A. & Mitrofanis, J. (2001) Evidence for a visual subsector within the zona incerta. *Visual Neurosci.*, **18**, 179–186.

Reichova, I. & Sherman, S.M. (2004) Somatosensory corticothalamic projections: distinguishing drivers from modulators. *J. Neurophysiol.*, **92**, 2185–2197.

Renart, A. & Machens, C.K. (2014) Variability in neural activity and behavior. *Curr. Opin. Neurobiol.*, **25C**, 211–220.

Sherman, S.M. (2001) Two types of thalamic relay. In Sherman, S.M. & Guillery, R.W. (Eds), *Exploring the Thalamus*. Academic Press, San Diego, pp. 229–247.

Sherman, S.M. & Guillery, R.W. (1996) Functional organization of thalamocortical relays. *J. Neurophysiol.*, **76**, 1367–1395.

Sherman, S.M. & Guillery, R.W. (2011) Distinct functions for direct and transthalamic corticocortical connections. *J. Neurophysiol.*, **106**, 1068–1077.

Shimegi, S., Ichikawa, T., Akasaki, T. & Sato, H. (1999) Temporal characteristics of response integration evoked by multiple whisker stimulations in the barrel cortex of rats. *J. Neurosci.*, **19**, 10164–10175.

Sobolewski, A., Kublik, E., Swiejkowski, D.A., Lęski, S., Kamiński, J.K. & Wróbel, A. (2010) Cross-trial correlation analysis of evoked potentials reveals arousal-related attenuation of thalamo-cortical coupling. *J. Comput. Neurosci.*, **29**, 485–493.

Sobolewski, A., Swiejkowski, D.A., Wróbel, A. & Kublik, E. (2011) The 5–12 Hz oscillations in the barrel cortex of awake rats - Sustained attention during behavioral idling? *Clin. Neurophysiol.*, **122**, 483–489.

Theyel, B.B., Llano, D.A. & Sherman, S.M. (2010) The corticothalamocortical circuit drives higher-order cortex in the mouse. *Nat. Neurosci.*, **13**, 84–88.

Trageser, J.C. & Keller, A. (2004) Reducing the uncertainty: gating of peripheral inputs by zona incerta. *J. Neurosci.*, **24**, 8911–8915.

Trageser, J.C., Burke, K.A., Masri, R., Li, Y., Sellers, L. & Keller, A. (2006) State-dependent gating of sensory inputs by zona incerta. *J. Neurophysiol.*, **96**, 1456–1463.

Urbain, N. & Deschênes, M. (2007) Motor cortex gates vibrissal responses in a thalamocortical projection pathway. *Neuron*, **56**, 714–725.

Veinante, P., Lavallée, P. & Deschénes, M. (2000) Corticothalamic projections from layer 5 of the vibrissal barrel cortex in the rat. *J. Comp. Neurol.*, **424**, 197–204.

Viaene, A.N., Petrof, I. & Sherman, S.M. (2011) Properties of the thalamic projection from the posterior medial nucleus to primary and secondary somatosensory cortices in the mouse. *Proc. Natl. Acad. Sci. USA*, **108**, 18156–18161.

Waite, P.M.E. (2004) Trigeminal sensory system. In Paxinos, G. (Ed.), *The Rat Nervous System*. Elsevier, New York, pp. 817–851.

Williams, M.N., Zahm, D.S. & Jacquin, M.F. (1994) Differential foci and synaptic organization of the principal and spinal trigeminal projections to the thalamus in the rat. *Eur. J. Neurosci.*, **6**, 429–453.

Wróbel, A., Kublik, E. & Musial, P. (1998) Gating of the sensory activity within barrel cortex of the awake rat. *Exp. Brain Res.*, **123**, 117–123.

Xing, D., Yeh, C.-I. & Shapley, R.M. (2009) Spatial spread of the local field potential and its laminar variation in visual cortex. *J. Neurosci.*, **29**, 11540–11549.